ISBN: 978-3-95450-230-1 ISSN: 2673-5350 doi:10.18429/JACoW-IBIC2021-MOPP31

Content from this work may be used under the terms of the CC BY 3.0 licence (© 2021). Any distribution of this work must maintain attribution to the author(s), title of the work, publisher, and DOI

PRELIMINARY STUDIES FOR THE SOLEIL UPGRADE BPM

M. El Ajjouri, N. Hubert, A. Gamelin, P. Alves, Synchrotron SOLEIL, 91192 Saint-Aubin, France

Abstract

Synchrotron SOLEIL is currently preparing a machine upgrade based on multibend achromat lattice with a drastically reduced horizontal electron beam emittance (<100 pm•rad). Foreseen quadrupole and sextupole strengths will impose a small vacuum chamber diameter and the future Beam Position Monitors (BPM) will have a 16 mm inner diameter (circular shape). To minimise the BPM contribution to the longitudinal impedance, and induced heating on their mechanics, the feedthrough and button shapes must be optimised. This paper summarises the systematic electromagnetic simulations that have been carried on in order to distinguish the effect of single dimension changes (such as button thickness and shape, ceramic thickness and diameter) on the amplitudes and frequency position of the resonances. It also introduces the preliminary BPM design for the SOLEIL upgrade project.

INTRODUCTION

Synchrotron SOLEIL has recently published the Conceptual Design Report (CDR) of the SOLEIL Upgrade [1]. The specifications are challenging for the new beam parameters especially the beam size and emittance below 100 pm rad (Fig. 1). The energy will remain the same as today (2.75 GeV). The project includes considerable modification of the accelerator and especially the replacement of the storage ring for a new multi bend achromat lattice. Natural bunch length will be 9 ps RMS, lengthened to 30 ps RMS by a harmonic cavity to preserve the transverse emittance and beam lifetime.

The main parameters of the SOLEIL upgrade SR and the existing SOLEIL SR are compared in Table 1.

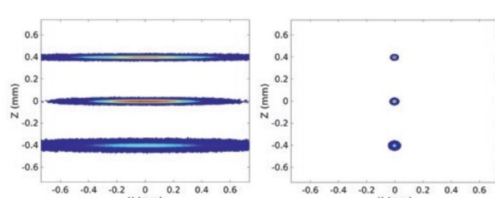

Figure 1: Comparison of the transverse beam profiles (x: horizontal, z: vertical plane) of the present SOLEIL (left) for 3 types of straight sections (short, medium and long / plots shifted for convenience) with 1% coupling and SOLEIL upgrade CDR reference lattice (right) with 50 pm.rad emittance.

Table 1: Main Parameters of the Present and CDR Reference Lattice

	SOLEIL	*SOLEIL Upgrade*
Circumference (m)	354.097	353.74
Beam energy (GeV)	2.75	2.75
maximum beam current (mA)	500	500
Natural emittance (pm.rad)	3900	80
Bunch length rms (ps)	15	9
BPM vacuum chamber (mm)	70/25	16
Number of BPM	122	~200

The SOLEIL upgrade project pushes the vacuum system conception to a new limit: the high gradient quadrupoles and the large strength of the sextupoles require the minimum size of the vacuum chamber inner diameter to be as low as 12 mm.

BPM SPECIFICATION AND CHALLENGING

The Beam Position Monitor (BPM) system is the largest (and one of the most critical) diagnostic systems for a synchrotron light source: about 200 position measurement units are considered in the CDR reference lattice. The system should deliver beam position measurement with a resolution of less than 50 nm RMS in closed orbit measurement (used for feedback loops). The measurement stability is also very important with a drift that must be below 1 µm over 24 hours. The BPM sensors for the SOLEIL upgrade will be the usual RF button pickups installed at 45° on the vacuum chamber. In order to protect the BPM from possible heating due to synchrotron radiation, its internal diameter is enlarged to 16 mm. The challenge will be the manufacturing of a small dimension pickup and its positioning on the BPM body with respect to tight tolerances in order to maintain an absolute position.

FIRST 2D SIMULATIONS

Preliminary studies have been carried out to design the future BPM pickups. With the usual delta over sum equation used to compute the position, the response is linear on a ± 1mm range around the BPM center with an on-axis error below 3 % (Fig. 2). We can consider a polynomial response to enlarge the linear range if needed for machine physics studies at large amplitude.

ISBN: 978-3-95450-230-1 ISSN: 2673-5350 doi:10.18429/JACoW-IBIC2021-MOPP31

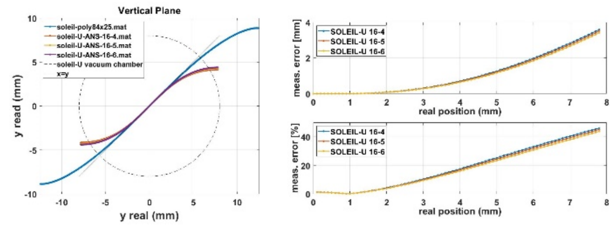

Figure 2: Linearity response for different button diameter (orange=4 mm, yellow=5 mm, purple=6 mm) compared to the current BPM in blue (left). Estimation of the error for the three diameters(right). BPMLab simulations [2].

The voltage collected on the antenna is related to the beam current by the Eq. (1) [3]:

$$U_{im}=Z_t(\omega,\beta)*I_{beam}=\left(\frac{1}{\beta c}\frac{A}{2\pi a}\right)*\frac{1}{C}*\frac{i\omega RC}{1+i\omega RC}*Ibeam \quad (1)$$

where a is the distance to the beam, A is the button area, β is the beam velocity and c is the speed of light.

The button capacitance to ground C and 50 Ω coaxial cable impedance R are equivalent to a high-pass filter with a cutoff frequency fcut =1/(2πRC). Hence the interest of maximising the value of the capacitance in order to have a lower cut-off frequency. The capacity C can be approximated by formula Eq. (2):

$$C=\frac{\pi\varepsilon_r t}{\ln(\frac{r_h}{r_b})}+\frac{\pi\varepsilon_r r_b{}^2}{d} \quad (2)$$

where t is the button thickness, ε_r is the dielectric permittivity, r_b and r_h the button and housing radius, and d is top button gap. The envisioned gap value of 200 µm is a compromise between the capacity and the constraints of mechanical manufacturing. The 3D numerical simulation computation with result using the CST electrostatic tool [4] allowed us to estimate the capacity of the button with complex design.

3D MODELISATION DESIGN AND OPTIMISATION

The power loss in the BPM block is one of the main parameters to be considered during its design. The BPM contribution to overall impedance budget has to be minimized and as well as the power deposited by the beam on the mechanics.

The power deposited by beam is given by formula Eq. (3) [5]:

$$P_{loss}=M*I_b^{2*}k_{loss} \quad (3)$$

where M is the number of bunches and I_b the beam current. The loss factor is given by Eq. (4):

$$k_{loss}=2M\sum_{p=0}^{\infty}R_e[Z_{||}(pM\omega_r)]*power\ spectrum(pM\omega_r) \quad (4)$$

where $\omega_r=2\pi f_{rev}$ and $R_e[Z_{||}(pM\omega_r)]$ is the real part of the longitudinal impedance.

The loss factor being the result of a convolution between the beam spectrum and the longitudinal impedance (see Fig. 3), it will be minimized by minimising amplitude of the impedance peaks or shifting them to high frequencies. Additional optimization can also be done avoiding that the impedance peaks falls at the same frequencies as the beam (discrete) spectrum.

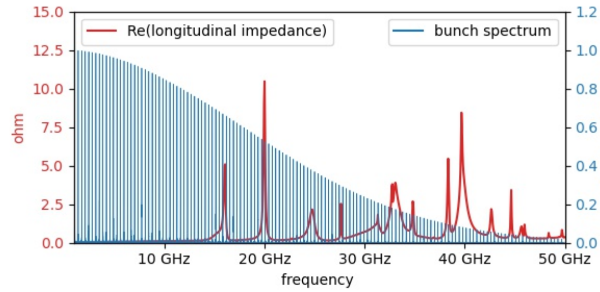

Figure 3: The longitudinal impedance (red) and beam spectrum (blue).

In this section we describe the main stages of optimisation of the different parts of the electrode to improve the longitudinal impedance, while preserving a maximum of signal transmitted by the button. Considered parameters for optimisation are presented in (Fig. 4)

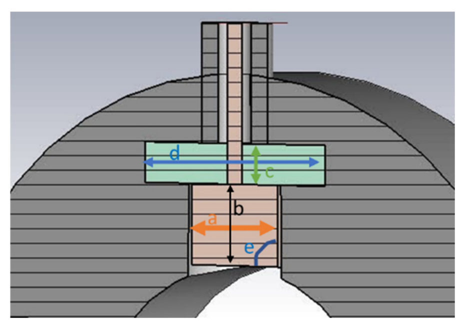

Figure 4: The parameters considered for optimisation: (a) button diameter, (b) button thickness, (c) dielectric thickness, (d) dielectric diameter and (e) button angle.

Button Diameter

Three button diameters are studied in order to find the best compromise between high signal collection (ie largest button surface) (Fig. 5) and lowest contribution to the longitudinal impedance (i.e. smallest diameter) (Fig. 6).

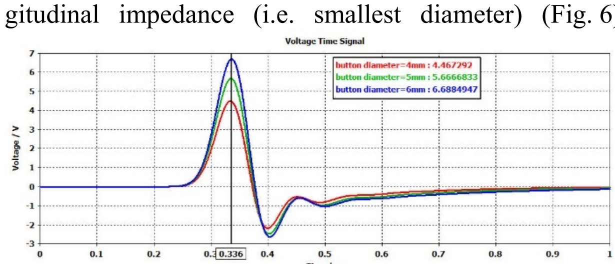

Figure 5: Voltage versus button diameter for bunch charge=1.44 nC and sigma =30 ps.

Content from this work may be used under the terms of the CC BY 3.0 licence (© 2021). Any distribution of this work must maintain attribution to the author(s), title of the work, publisher, and DOI

ISBN: 978-3-95450-230-1 ISSN: 2673-5350 doi:10.18429/JACoW-IBIC2021-MOPP31

Content from this work may be used under the terms of the CC BY 3.0 licence (© 2021). Any distribution of this work must maintain attribution to the author(s), title of the work, publisher, and DOI

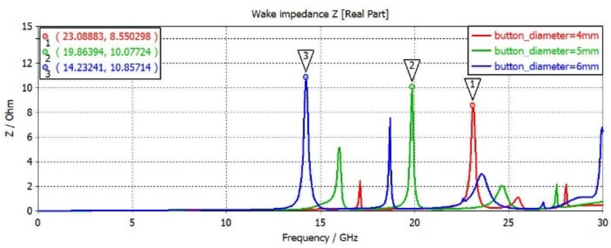

Figure 6: Real part of longitudinal impedance versus button diameter.

The first trapping mode, corresponding to the TE_{11}, mode is given by the Eq. (5) [6, 7], it depends on the diameter of the button, and it's housing.

$$f_c^{Hmp} = \frac{1}{\sqrt{\varepsilon_r}} * \frac{c}{\pi} * \frac{1}{r_b + r_h} \quad (5)$$

where ε_r is the dielectric permittivity, r_b and r_h the button and housing radius. This analytical evaluation of TE_{11} mode is compared to the CST simulation [2] in Table 2 for the three diameters considered.

Table 2: Comparison Between Analytical Model and the TE11 Mode Frequency Computing by CST

Button diameter (mm)	4	5	*6*
Analytical value (GHz)	22,72	18,35	*15,39*
Numerical computing (GHz)	23.14	19.85	*14.24*

Analytical value and numerical computing are in good agreement. The difference may come from the numerical model that takes into account the complete feedthrough and not only the button geometry.

The 5 mm diameter presents the good compromise between the signal amplitude and impedance contribution.

Button Thickness

We study the effect of the button thickness to reduce the heating induced by the beam on the BPM button. The observation of the impedance spectrum shows that the thickness of 2 mm presents a larger peak towards 15 GHz (Fig 7).

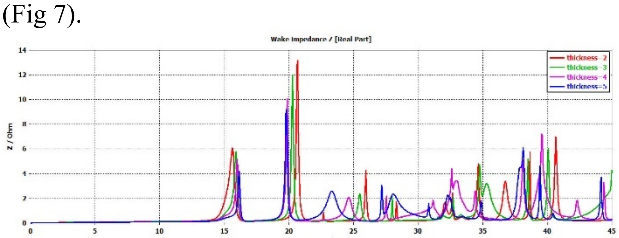

Figure 7: Real part of longitudinal impedance versus button thickness.

According to Eq. (3), the minimum power is obtain for 4 mm button thickness, as summarized in Table 3.

Table 3: Power Loss Versus Button Diameter (mm) for Sigma Beam Length = 9 ps rms

Button thickness (mm)	2	3	4	5
Power loss (W)	6,13	5.14	4.91	5.58

Dielectric Optimisation

The thickness, the relative permittivity, the diameter and the pin radius of the dielectric influence directly the frequency of trapped modes due to the ceramic (or other dielectric). The frequency of this mode can be estimated by Eq. (6) [7].

$$f^{Hm1p} = \frac{1}{\sqrt{\varepsilon r}} * \frac{c}{2\pi} * \sqrt{\left(\frac{2m}{r_p + r_d}\right)^2 + \left(\frac{\pi p}{t_d}\right)^2} \quad (6)$$

where ε_r is relative permittivity , r_d dielectric radius, r_p pin radius and t_d the dielectric thickness m and p=1,2,3….
In our case we consider Al_2O_3 alumina with ε_r=9.4.

We simulated several thicknesses of the dielectric. (Fig. 8) shows the longitudinal impedance for different thicknesses.

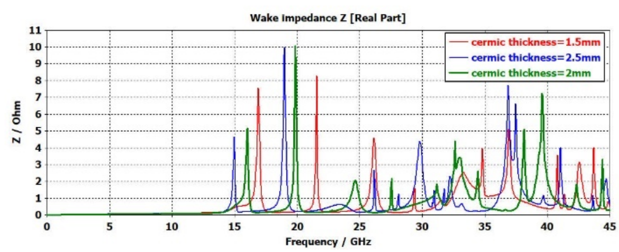

Figure 8: real part of longitudinal impedance vs. ceramic thickness. Red 1.5 mm, green 2 mm and blue 2.5 mm.

We expected that the thickness of the ceramic does not influence the first peak, which depends only on the geometry of the button. We see that all the spectrum shifts in high frequency when the thickness of the ceramic is reduced. This is also probably due to the fact that the numerical computing consider the whole feedthrough geometry and not only the part around the ceramic. The calculation of the beam power shows that a thickness of 2 mm is the best compromise and will be chosen for our design (see Table 4).

Table 4: H111 Mode Frequency Versus Ceramic Thickness

Ceramic thickness (mm)	1.5	2	2.5
Analytical value (GHz)	33.69	25.89	21.33
Numerical computing (GHz)	21.55	19.86	18.99
Power loss (W)	5,75	4,91	5,24

The dielectric diameter is usually adapted to the pin diameter to respect the 50 Ω impedance of the feedthrough and to optimise the signal transmission between button and coaxial cable. Such constraint would impose a big dielectric diameter, and a big feedthrough difficult to implement

ISBN: 978-3-95450-230-1 ISSN: 2673-5350 doi:10.18429/JACoW-IBIC2021-MOPP31

in the 16 mm BPM. Simulation on a mis adapted feed-through (with smaller dielectric diameter) is possible and even improves a little bit the amplitude of the collected signal (Fig. 9).

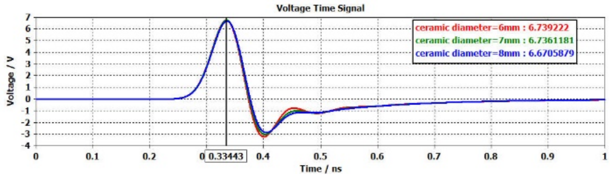

Figure 9: Time signal induced by with 30 ps rms bunch length and 1.44 pC bunch charge against ceramic diameter red 6 mm, blue 7 mm and green 8 mm.

Button Geometry Effect

Based on the work carried out on the optimisation of the BPM impedance of Sirius [7], we compared three shapes of buttons: with angles of 90°, 75°, and 65° (Fig. 10).

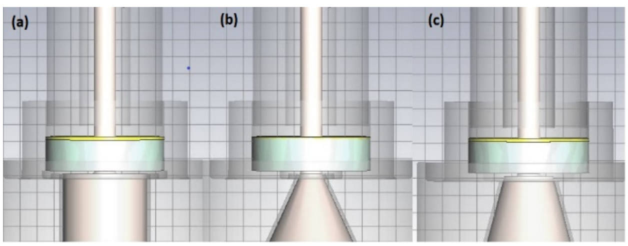

Figure 10: Button angle shape simulates (a) Button 90° (b) 65° conical button. (c) 75° conical button.

The conical shape of the button shifts the trapped mode in the high frequencies (Fig. 11).

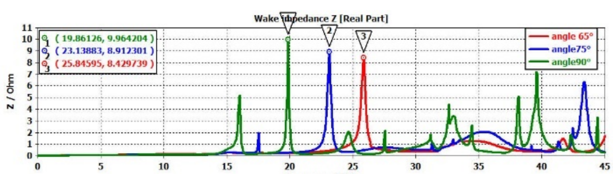

Figure 11 The real part of longitudinal impedance for different button geometry: green 90° button angle, blue 75° button angle, red 65° button angle.

As a consequence, the power deposed by the beam on the BPM block is decreased. With bunch length equals 9 ps rms, the power drops from 20% between the 90° button angle and the 65°button angle (see Table 5).

Table 5: Power Loss Versus Button Angle

Button angle in degree	65	75	90
power loss (w)	3,93	4.25	4.91

PROTOTYPING

In order to validate the mechanical integration of such a small design (initial internal diameter was even smaller at 10 mm) and BPM calibration procedure, we have realised a first prototype with commercially available feedthroughs (3 mm buttons) (see Fig. 12).

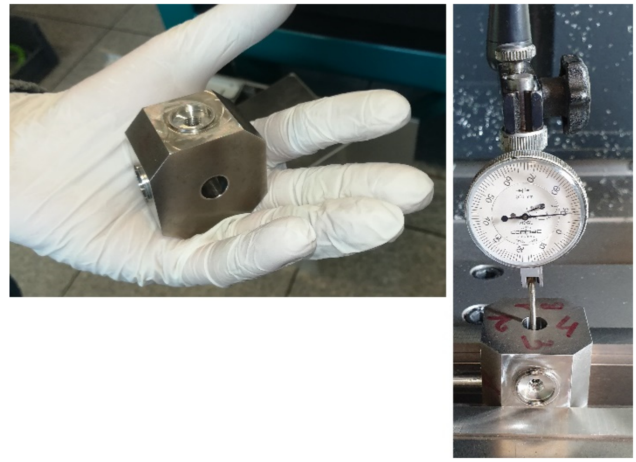

Figure 12: BPM prototype (left) and electrode positioning metrology (right).

Careful metrology has been carried on in order to optimize the mechanical tolerances to be defined for the BPM and feedthrough manufacturing.

PERSPECTIVES

A preliminary discussion with the button manufacturers made it possible to raise and resolve several blocking points such as the mechanical positioning of the buttons or the mechanical tolerances.

A new button design is being validated, and a new prototype is being manufactured. Thermal simulation has still to be conducted to decide the materials for the BPM body and button, and if a cooling system will be required.

CONCLUSION

Future BPMs for the SOLEIL upgrade are under design. The main challenge is the drastic reduction of the vacuum chamber circumference. Accurate electromagnetic simulations are ongoing to minimise impedance. Deposited power should also be estimated, and thermal simulation will help us to decide whether to have a water-cooling circuit around the body of the BPM.

REFERENCES

[1] Synchrotron SOLEIL "Conceptual Design Report", https://www.synchrotron-soleil.fr/en/file/13803/download?token=OUzsp46P

[2] A. A. Nosych, U. Iriso, and J. Olle, "Electrostatic Finite-element Code to Study Geometrical Nonlinear Effects of BPMs in 2D", in *Proc. 4th Int. Beam Instrumentation Conf. (IBIC'15)*, Melbourne, Australia, Sep. 2015, pp. 418-422. doi:10.18429/JACoW-IBIC2015-TUPB047

[3] P. Forck, P. Kowina, and D. Liakin, GSI, "Beam Position Monitors", CAS, Dourdan, France, May 2008.

[4] https://www.3ds.com/fr/produits-et-services/simulia/produits/cst-studio-suite

[5] L. Teofili *et al.*, "A Multi-Physics Approach to Simulate the RF Heating 3D Power Map Induced by the Proton Beam in a Beam Intercepting Device", in *Proc. 9th Int. Particle Accelerator Conf. (IPAC'18)*, Vancouver, Canada, Apr.-May 2018, pp. 3452-3455. doi:10.18429/JACoW-IPAC2018-THPAK093

Content from this work may be used under the terms of the CC BY 3.0 licence (© 2021). Any distribution of this work must maintain attribution to the author(s), title of the work, publisher, and DOI

ISBN: 978-3-95450-230-1 ISSN: 2673-5350 doi:10.18429/JACoW-IBIC2021-MOPP31

[6] A. Blednykh *et al*., "NSLS-II Storage Ring BPM Button Development", in *Proc. 6th Int. Particle Accelerator Conf. (IPAC'15)*, Richmond, VA, USA, May 2015, pp. 748-750. doi:10.18429/JACoW-IPAC2015-MOPMN021

[7] H. O. C. Duarte, S. R. Marques, and L. Sanfelici, "Design and Impedance Optimization of the SIRIUS BPM Button", in *Proc. 2nd Int. Beam Instrumentation Conf. (IBIC'13)*, Oxford, UK, Sep. 2013, paper TUPC07, pp. 365-368.

Content from this work may be used under the terms of the CC BY 3.0 licence (© 2021). Any distribution of this work must maintain attribution to the author(s), title of the work, publisher, and DOI